Ultrafast photoinduced conductivity reduction by bonding orbital control in an incommensurate crystal

M. Lejman,[1] M. Weis,[1] N. Nilforoushan,[1] J. Faure,[1] V. Ta Phuoc,[2] L. Cario,[3] and D. Boschetto[1,*]

[1]*Laboratoire d'Optique Appliquée, ENSTA Paris, CNRS, Ecole Polytechnique, Institut Polytechnique de Paris, 91761 Palaiseau, France*

[2]*GREMAN UMR 7347 CNRS, Université de Tours, INSA CVL, Parc Grandmont, 37200 Tours, France*

[3]*Nantes Université, CNRS, Institut des Matériaux de Nantes Jean Rouxel, IMN, F-44000 Nantes, France*

(Received 6 May 2022; revised 12 September 2023; accepted 19 September 2023; published 12 October 2023)

In this paper, we demonstrate the ultrafast reduction of conductivity in an incommensurate crystal structure within hundreds of femtoseconds. This phenomenon stands in stark contrast to most prior experimental investigations where incident light pulses led to increased conductivity. We achieve this by selectively targeting a specific atomic bond using near-infrared light pulses. Our investigation focuses on misfit layered chalcogenide $(LaS)_{1.196}VS_2$, known as $LaVS_3$, a semimetal with incommensurability along one crystallographic direction. Our time-resolved electron dynamics investigation reveals that the conductivity decreases as photoexcited electrons are promoted into localized energy states within vanadium clusters due to the incommensurate structure. These findings offer insights into the potential for controlling electronic properties at femtosecond time scales, with implications for the development of ultrafast electronic devices.

DOI: 10.1103/PhysRevB.108.134306

I. INTRODUCTION

The ability to precisely manipulate the physical properties of materials on femtosecond time scales holds promise for revolutionary advancements in ultrafast electronics. This frontier of research relies on harnessing femtosecond light pulses to selectively control specific electronic or phononic excitations within materials, a feat demonstrated in various studies [1–7]. The choice of light wavelength becomes pivotal, as it dictates the specific excitation that can be addressed, be it electronic [8] or phononic [3,9]. The ability to control the conductivty state of a material on an ultrafast time scale emerges as a focal point of these investigations [2–4,7,10–15]. Authors of numerous studies have highlighted the potential to increase conductivity through photoexcitation, effectively modulating or transiently collapsing the electronic band gap [16–18]. However, the quest for ultrafast electronics depends on the ability to switch between conducting and nonconducting states. While authors of extensive research have explored the photoinduced increase in conductivity, only a few authors have explored the converse possibility on short time scales [19,20]. In this search of inducing a reduction in conductivity through photoexcitation, incommensurate materials emerge as particularly promising candidates. Incommensurability introduces a modulation of interatomic distances within the crystal structure, leading to the formation of localized states like disorder-induced states in Anderson localization [21,22]. Exciting electrons within these localized states offers a unique opportunity to lower and potentially inhibit the conductivity of the crystal.

In this paper, we focus on the investigation of the ultrafast response of $LaVS_3$, a misfit layered compound, to near-infrared spectral excitation using time-resolved pump-probe spectroscopy. Our results unveil the photoinduced reduction of free carrier density, a phenomenon effectively explained through density functional theory (DFT) calculations, interband rate equations, and the two-temperature model. Under the influence of specific near-infrared wavelengths, electrons are excited and subsequently trapped in the localized energy states of vanadium clusters, resulting in a reduction of electric conductivity. This experimental evidence establishes the presence of these localized states within the vanadium clusters and advances our understanding of ultrafast control over material properties.

The misfit layered compound $(LaS)_{1.196}VS_2$, abbreviated as $LaVS_3$, has a composite structure which results from a regular stacking of [LaS] (rock-salt type structure) and $[VS_2]$ (CdI_2-type structure) layers along the c direction [23] (for review articles, see also Refs. [24,25]). This material exhibits an incommensurability (= lattice mismatch) along the in-plane a axis which has a huge impact on the vanadium distances observed within the VS_2 layer. The incommensurate composite nature gives rise to two major features: on one hand, the electrons are confined within the layers, and therefore, they reveal a quasibidimensional character; on the other hand, the V-V distances are modulated along the crystallographic a direction, giving rise to vanadium clusters. Figure 1 shows the pattern formed by the vanadium atoms separated by the lowest distances (<3.25 Å), drawn using a commensurate approximation. One-dimensional zigzag clustering of the vanadium atoms is clearly visible. This implies the existence of domains in which the V-V distance gets smaller, forming vanadium clusters. It has been suggested that such clusters form localized states for electrons, which affects the conductivity of the compound [26–32]. However, no experimental evidence of the formation of these localized states has been reported, which motivated our investigation.

*Davide.Boschetto@ensta.fr

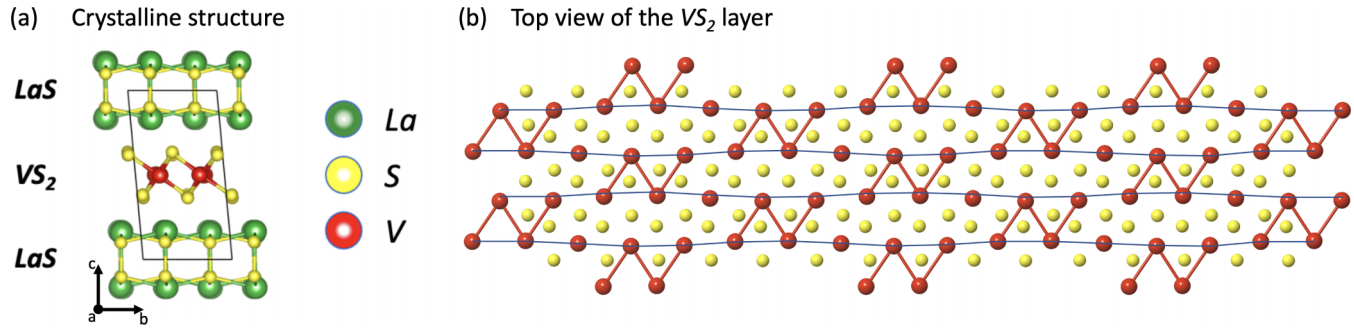

FIG. 1. (a) Crystal structure of $LaVS_3$, composed by stacking of LaS and VS_2 slabs, respectively. (b) Top view of the VS_2 layer, showing a periodic change in the interatomic V-V distance. The four closest vanadium neighbors, linked for clarity by a red solid line, form a vanadium cluster.

II. EXERIMENTAL RESULTS

Figures 2(a)–2(c) show the transient changes of reflectivity ($\Delta R/R$) of $LaVS_3$ vs the pump-probe time delay at a few selected fluences, corresponding to pump and probe pulses centered at wavelengths of 1.2 μm (1 eV) and 2.4 μm (0.5 eV), respectively. The behavior is characterized by an abrupt increase of the reflectivity, followed by relaxation until a plateau is reached. Right after the arrival of the pump pulse, the reflectivity increases up to ∼200 fs. Once the maximum is reached,

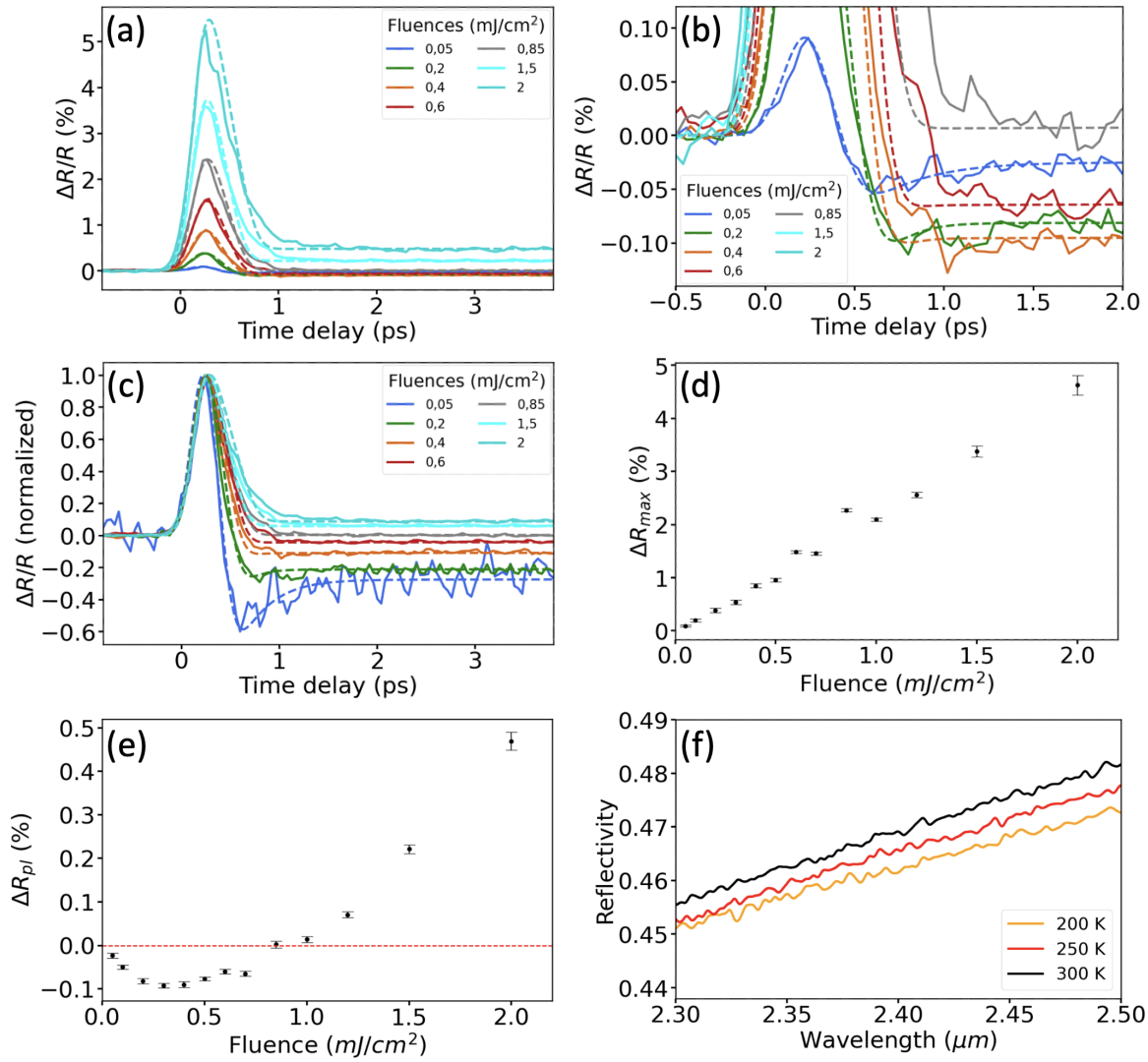

FIG. 2. [(a)–(c)] Transient reflectivity (solid line) and simulated reflectivity (dashed line) of $LaSV_3$ crystal at room temperature as a function of the pump fluence for pump 1.2 μm (1 eV) and probe 2.4 μm (0.5 eV) wavelength. (d) and (e) ΔR_{max} and ΔR_{pl} vs pump fluence. (f) Reflectivity from ellipsometry measurement at equilibrium vs crystal temperature, in the spectral range from 2.3 to 2.5 μm.

we clearly observe that the subsequent decay of the reflectivity depends on the pump fluence. For low pump fluences (<0.85 mJ/cm^2), the transient reflectivity continues to drop, acquires a negative sign, and after reaching a minimum ($\sim$500 fs), it finally exhibits slow relaxation dynamics toward equilibrium. Conversely, this twofold feature in the ultrafast dynamics disappears by increasing the excitation density. For instance, for a pump fluence of 2 mJ/cm^2, after 200 fs, the dynamics shows an exponentiallike decay. In both cases, the relaxation back to the equilibrium state occurs when electrons evacuate their excess energy to the lattice thanks to electron-phonon coupling [33]. Therefore, after photoexcitation, the lattice heats up, and the value of the transient reflectivity at the plateau should be proportional to the electron-phonon equilibration temperature.

Figures 2(d) and 2(e) show the maximum value of $\Delta R/R$ (named ΔR_{max}) and the value of $\Delta R/R$ at the plateau (named ΔR_{pl}) vs pump fluence. The values of ΔR_{max} have been estimated using a Gaussian fit, while ΔR_{pl} has been calculated as the average of the $\Delta R/R$ between 2.5 and 4 ps. While we observe a linear behavior of ΔR_{max} vs fluence, we notice that ΔR_{pl} is not a monotonic function of the pump fluence. Indeed, ΔR_{pl} decreases and reaches a minimum negative value at $\approx$0.4 mJ/cm^2 and then increases and acquires a positive sign above $\approx$0.85 mJ/cm^2.

Here, ΔR_{max} is proportional to the number of photoexcited electrons and represents a transient increase of the conductivity. As such, it should vary linearly as a function of the pump fluence, in agreement with Fig. 2(d). On the other hand, ΔR_{pl} should be proportional the lattice temperature T_L (neglecting both thermal and electron diffusion), and therefore, its value should always increase for all fluences. Instead, as observed in Fig. 2(e), the behavior of ΔR_{pl} is nonmonotonic and acquires a sign change below and above $\approx$0.85 mJ/cm^2. This gives evidence of a nontrivial process triggered by ultrafast excitation of electrons when pumped at photon energy of 1 eV.

We can roughly estimate the final lattice temperature by the conservation of energy and neglecting diffusion, which for a pump pulse of 1 mJ/cm^2 would give an increase of $\sim$26 K (see Supplemental Material [34] for more details). As the energy deposited by the pump pulse finally heats the sample, we should expect that the reflectivity always increases for all fluences, in contrast with what we have experimentally observed. To estimate the changes of the reflectivity vs temperature at equilibrium, we performed ellipsometry measurements at three sample temperatures [shown in Fig. 2(f)]. Here, we clearly observe that the reflectivity always increases with the temperature. Therefore, the transient state at lower fluences corresponds to a nonthermal state. Indeed, by lowering the fluence, both ΔR_{max} and ΔR_{pl} should go to zero, but they should never change their signs. The behavior of ΔR_{pl} vs fluence demonstrates that there is competition between two different mechanisms involved in this dynamics.

III. DISCUSSION

These results are well explained by a reduction of the electrical conductivity due to the transition of the photoexcited electrons into the localized states of the vanadium clusters generated by the incommensurability of the crystal structure. To better understand the impact of this clustering on the electronic structure, we have therefore performed DFT calculations considering the modulation of the structure of $LaVS_3$ at 300 K [see Fig. 3(a)]. These calculations show that the $3d$ levels of vanadium are split into t_{2g} and e_g levels and that the main contribution around the Fermi level is given by the t_{2g} orbitals. These calculations also reveal, as the most striking difference compared with previous work [28] (performed without modulation), a more pronounced splitting of the t_{2g} bands in three subbands. As shown in Fig. 3(b), representing the partial density of states (DOS) of the vanadium atom, the three subbands result from the split of d_{yz} and d_{xz} orbitals, while the d_{xy} remains unsplit.

This splitting comes from the clustering of the vanadium atoms which is now considered in the calculation. In the structure of $LaVS_3$, all vanadium atoms indeed interact to form an incommensurate zigzag bonding pattern [Fig. 1(b)]. Taking as reference axes the x, y, and z directions pointing toward the sulfur ligands within the octahedral surrounding of the vanadium atoms, the direction of the shortest V-V distances implies that mostly the d_{yz} or d_{xz} orbitals could interact to form σ-type bonding. A calculation on a V_2S_{10} set of atoms extracted from the real structure and exhibiting only a single V-V bond demonstrates that this σ-type interaction can lift the degeneracy of the t_{2g} orbitals by >1 eV (see Supplemental Material [34]). It means that the incommensurate σ-type bonding pattern lifts the degeneracy of the t_{2g} bands in bonding $\sigma(d_{yz};d_{xz})$, antibonding $\sigma^*(d_{yz};d_{xz})$, and nonbonding d_{xy} levels, as represented in Fig. 3(c). This splitting explains very well the subbands observed in our calculation for the projected DOS of a single or all vanadium atoms of the modulated structure [see Figs. 3(a) and 3(b)]. According to these calculations, a pump photon of 1 eV only affects the t_{2g} bands. It allows either a bonding $\sigma(d_{yz};d_{xz})$ to nonbonding d_{xy} transition, or a nonbonding d_{xy} to antibonding $\sigma^*(d_{yz};d_{xz})$ transition, represented by two blue arrows in Fig. 3(c), respectively. We also point out that the $\sigma(d_{yz},d_{xz}) \rightarrow d_{xy}$ transition is from bonding to nonbonding states, which will favor a declusterization thanks to the increase of the shortest V-V distances.

The partially filled d_{xy} level corresponds to a conduction band, and therefore, the transition $\sigma(d_{yz},d_{xz}) \rightarrow d_{xy}$ will increase the electrical conductivity of the crystal. Instead, the σ^* state corresponds to a localized state within the vanadium clusters, and therefore, the transition $d_{xy} \rightarrow \sigma^*(d_{yz},d_{xz})$ will decrease the electrical conductivity of the crystal. Therefore, the pump pulse will favor a declusterization [$\sigma(d_{yz},d_{xz}) \rightarrow d_{xy}$ transition] and can remove some DOS at the Fermi level toward the localized states [$d_{xy} \rightarrow \sigma^*(d_{yz},d_{xz})$ transition]. These two excitation processes are in competition, and the final sign of the reflectivity change will be given by the balance between them.

The temporal behavior of the reflectivity can be described by considering the dependence on both the occupation of the d_{xy} level, named $n_{d_{xy}}(t)$, as well as on the lattice temperature T_L:

$$\Delta R(t) = \alpha \Delta n_{d_{xy}}(t) + \beta \Delta T_L(t). \quad (1)$$

Here, $n_{d_{xy}}(t)$ represents the average electron density per vanadium in the d_{xy} band, which is the conduction band. We

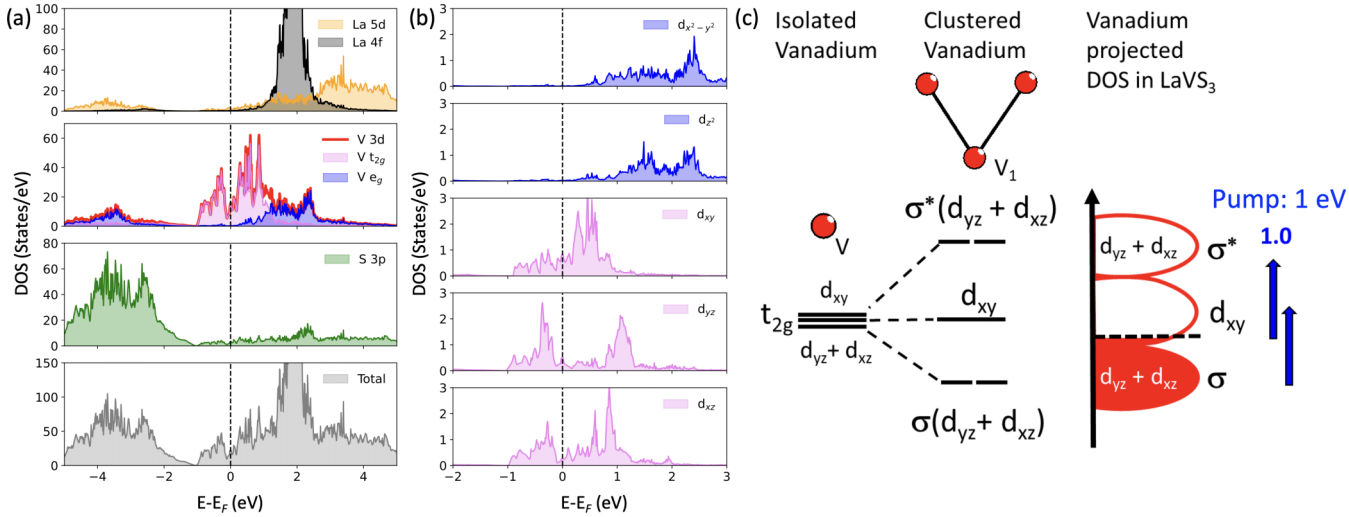

FIG. 3. Theoretical calculation and bond orbitals in $LaVS_3$. (a) Density of states (DOS) calculation of $LaVS_3$, showing that the $3d$ levels of vanadium are split into t_{2g} and e_g levels and that the main contribution around the Fermi level is given by the t_{2g} orbitals. (b) Partial DOS of vanadium, showing the formation of three subbands resulting from the split of d_{yz} and d_{xz} orbitals, while d_{xy} remains unsplit. (c) Energy splitting in the $LaVS_3$ structure for the vanadium atoms in the cluster and accessible interband transitions with a photon energy of ∼1 eV, shown by the blue arrows.

remark that the dependence of the reflectivity on the electron temperature can be neglected because $LaVS_3$ is a semimetal with low electron density at equilibrium. Therefore, the changes in reflectivity are dominated by the modifications of the carriers density rather than their energy distribution within the conduction band, in contrast with pure metallic behavior.

The temporal behavior of $n_{d_{xy}}(t)$ can be calculated using rate equations between the occupation levels of the three bands, namely, $n_\sigma(t)$, $n_{d_{xy}}(t)$, and $n_{\sigma^*}(t)$:

$$\begin{aligned}
\frac{d}{dt}n_\sigma(t) &= c_{21}n_{d_{xy}}(t) + c_{31}n_{\sigma^*}(t) - S_{12}(t),\\
\frac{d}{dt}n_{d_{xy}}(t) &= -c_{21}n_{d_{xy}}(t) + c_{32}n_{\sigma^*}(t) + S_{12}(t) - S_{23}(t),\\
\frac{d}{dt}n_{\sigma^*}(t) &= -c_{32}n_{\sigma^*}(t) - c_{31}n_{\sigma^*}(t) + S_{23}(t),
\end{aligned} \tag{2}$$

where the relaxation rate constants c_{21}, c_{31}, and c_{32} concern the transitions $n_\sigma \leftrightarrow n_{d_{xy}}$, $n_\sigma \leftrightarrow n_{\sigma^*}$, and $n_{d_{xy}} \leftrightarrow n_{\sigma^*}$, respectively, and S_{12} and S_{23} are the source terms (with Gaussian shape) for the excitation processes $n_\sigma \rightarrow n_{d_{xy}}$ and $n_{d_{xy}} \rightarrow n_{\sigma^*}$, respectively.

On the other hand, the changes in both the electron temperature T_e and lattice temperature T_L are calculated by the two-temperature model [35] (see Supplemental Material [34] for more details), where the thermal energy rate exchange is governed by the electron-phonon coupling factor g.

According to this model, the peak of the reflectivity is due to the increase of the number of electrons excited into the d_{xy} band. After the electronic peak is reached, the decrease of the transient reflectivity is due to the emptying of the d_{xy} band. However, as part of the electrons are excited into the long-living localized state σ^*, the final value of the electron density in the d_{xy} band is below the initial value, which implies a negative value of $\Delta R/R$. Figure 4 shows an example of the transient behavior of the occupation levels of the three bands for a selected fluence of 2 mJ/cm^2. We notice that, while the excess electrons pumped into the d_{xy} band relax to recombine with the holes in the σ band, the electrons pumped into the σ^* band are trapped in a very long-living state.

On the other hand, the increase of the lattice temperature produces a positive change of $\Delta R/R$ [Fig. 2(f)]. Therefore,

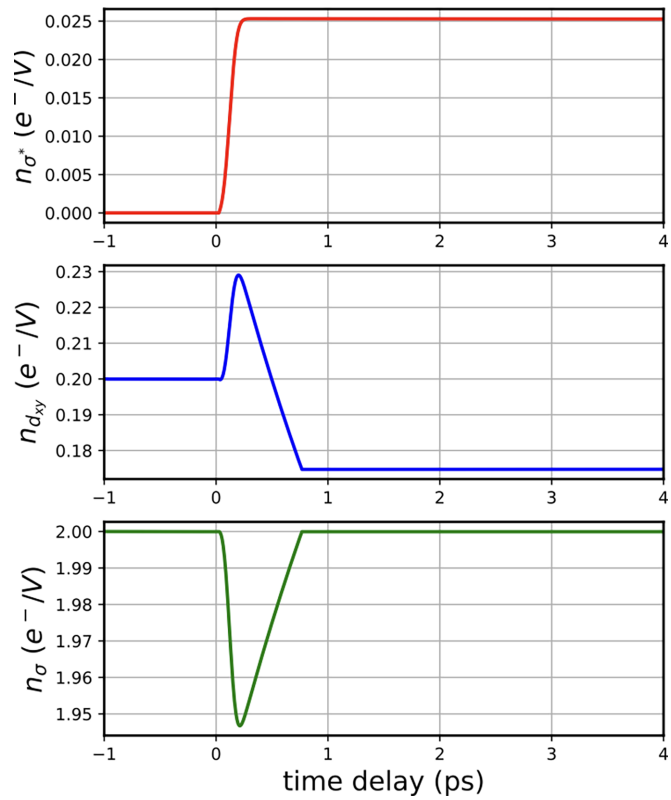

FIG. 4. Occupation level of the σ, d_{xy}, and σ^* orbitals vs time delay for a pump fluence of 2 mJ/cm^2.

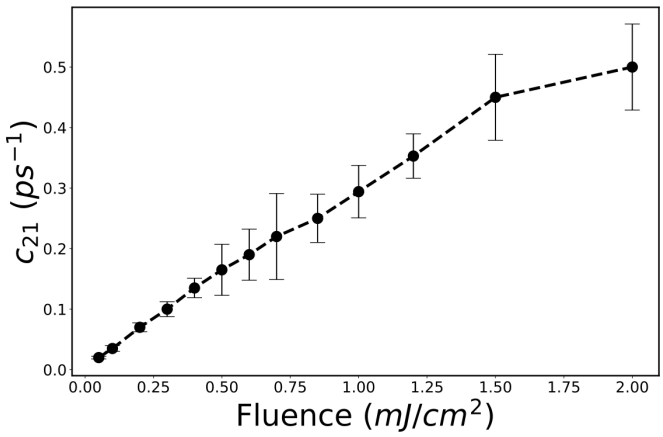

FIG. 5. c_{21} decay rate from the d_{xy} to the σ orbital vs pump fluence.

the value of the transient reflectivity at the plateau depends on the competition between these two processes. At low fluence, as the thermal contribution to the reflectivity change is small, $\Delta R_{\rm pl}$ is dominated by the reduction of the electrons in the d_{xy} band, resulting in negative values. Instead, at higher fluence, the lattice heating dominates, resulting in a positive value of $\Delta R_{\rm pl}$. This can explain the nonmonotonic behavior and the change of sign shown in Fig. 2(e).

The results of this fitting procedure are shown in Figs. 2(a)–2(c) as dashed lines and are found to be in excellent agreement with the experimental results. Here, we arbitrarily kept the rate coefficients c_{31} and c_{32} at constant value 4×10^{-4} ps^{-1}, whereas the rate coefficient c_{21}, the electron-phonon coupling factor g, and the coefficients α and β are left as free parameters. From the fit, we found $\alpha = 1.6 \pm 0.4$ and $\beta = (7 \pm 1) \times 10^{-4}$ K^{-1}. This value of β is in agreement with the equilibrium reflectivity measurements vs temperature shown in Fig. 2(f), from which we extract $\beta \approx 6 \times 10^{-4}$ K^{-1}. Fluctuations on the values of the coefficients α and β are due to the errors in the estimation of the pump fluence. Instead, the values of both c_{21} and g are found to increase with fluence, as shown in Figs. 5 and S5 in the Supplemental Material [34], respectively. The rate coefficient c_{21} increases nearly linearly with the fluence. This dependence can be explained by remembering that increasing the fluence favors the declusterization, which restores a more pronounced metallic character in which the electron-hole recombination is faster, and therefore, the relaxation rate c_{21} has a higher value. On the other hand, the increase of the g factor can be explained by noting that the electron-phonon coupling increases with the lattice temperature, and therefore, higher fluence leads to higher electron-phonon energy transfer.

It is important to note that, for lower pump photon energy of 0.73 eV (corresponding to a wavelength $\lambda = 1700$ nm), we did not observe any sign modification of $\Delta R_{\rm pl}$ (see Fig. S13 in the Supplemental Material [34]). This is in good agreement with our explanation, as a lower pump photon energy cannot induce the $d_{xy} \rightarrow \sigma^*(d_{yz}, d_{xz})$ transition and can only induce the $\sigma(d_{yz}, d_{xz}) \rightarrow d_{xy}$ transition, which corresponds to a higher conductivity state and a positive reflectivity change.

We point out here that the lower reflectivity state at low fluence has a nonthermal character, as the reflectivity should increase as a function of the temperature [Fig. 2(f)], and that such a nonthermal state lasts for >100 ps (see Supplemental Material [34] for more details). Such a long-living nonthermal state is very unusual and is related to the relaxation dynamics of the declusterization.

The dynamics of both clusterization and declusterization, involving the changes of the V-V bonds, must be further investigated by time-resolved electron or x-ray diffraction, which are more sensitive to the interatomic distances. We should expect the clusterization to be accompanied by a stiffening of V-V phonon modes, as already observed on other vanadium-based crystals (V_2O_3) using several time-resolved techniques [8,36].

IV. CONCLUSIONS

In conclusion, our investigation shows a remarkable light-induced ultrafast nonthermal transient reduction in conductivity in a $LaVS_3$ crystal, driven by the transfer of electrons into localized states within vanadium clusters that are generated by the incommensurability of the crystal structure. These findings provide compelling evidence for the presence of such localized trapped states within these clusters. The transient behavior of reflectivity observed in this paper finds a comprehensive explanation through a synergy of theoretical tools, including DFT calculations, rate equations, and the two-temperature model. Our analysis reveals that this transient reflectivity phenomenon arises from the interplay between two key mechanisms: the alteration of electron density within the conduction band, influenced by the population of electrons in the trapped states of vanadium clusters, and the concurrent thermal lattice heating. These results shine light on the use of the localized states within the clusters in incommensurate systems as a possible way to control the conductivity properties of solids on ultrafast time scales.

ACKNOWLEDGMENTS

The authors gratefully thank M. Filoche for his careful reading of the paper as well as for his comments and constructive discussions. This paper has been supported by the Region Ile-de-France in the framework of the SESAME Electrophonon project (Grant No. 14014520). We acknowledge the financial support from the French Department of Defense (DGA) in the frame of the Oscillateur térahertz Project (Grants No. 2015.60.0006.00.470.75.01 and No. 2018 60 0071 00 470 75 01) as well as PALM in the framework of the TPS grant (Grant No. ANR-10-LABX-0039-PALM) and Laserlab-Europe (No. EU- H2020 654148).

[1] E. Collet, M.-H. Lemée-Cailleau, M. Buron-Le Cointe, H. Cailleau, M. Wulff, T. Luty, S.-Y. Koshihara, M. Meyer, and S. Techert, Laser-induced ferroelectric structural order in an organic charge-transfer crystal, Science **300**, 612 (2003).

[2] A. Cavalleri, T. Dekorsy, H. H. W. Chong, J. C. Kieffer, and R. W. Schoenlein, Evidence for a structurally-driven insulator-to-metal transition in VO_2: A view from the ultrafast timescale. Phys. Rev. B **70**, 161102(R) (2004).

[3] M. Rini, R. Tobey, N. Dean, J. Itatani, Y. Tomioka, Y. Tokura, R. W. Schoenlein, and A. Cavalleri, Control of the electronic phase of a manganite by mode-selective vibrational excitation, Nature (London) **449**, 72 (2007).

[4] W. Hu, S. Kaiser, D. Nicoletti, C. R. Hunt, I. Gierz, M. C. Hoffmann, M. Le Tacon, T. Loew, B. Keimer, and A. Cavalleri, Optically enhanced coherent transport in $YBa_2Cu_3O_{6.5}$ by ultrafast redistribution of interlayer coupling, Nat. Mater. **13**, 705 (2014).

[5] X. Li, T. Qiu, J. Zhang, E. Baldini, J. Lu, A. M. Rappe, and K. Nelson, Terahertz-field-induced ferroelectricity in quantum paraelectric $SrTiO_3$, Science **364**, 1079 (2019).

[6] M. Schneider, B. Pfau, C. M. Günther, C. von Korff Schmising, D. Weder, J. Geilhufe, J. Perron, F. Capotondi, E. Pedersoli, M. Manfredda *et al.*, Ultrafast demagnetization dominates fluence dependence of magnetic scattering at Co *M* edges, Phys. Rev. Lett. **125**, 127201 (2020).

[7] J. W. McIver, B. Schulte, F.-U. Stein, T. Matsuyama, G. Jotzu, G. Meier, and A. Cavalleri, Light-induced anomalous Hall effect in graphene, Nat. Phys. **16**, 38 (2020).

[8] G. Lantz, B. Mansart, D. Grieger, D. Boschetto, N. Nilforoushan, E. Papalazarou, N. Moisan, L. Perfetti, V. L. R. Jacques, D. Le Bolloc'h *et al.*, Ultrafast evolution and transient phases of a prototype out-of-equilibrium Mott-Hubbard material, Nat. Commun. **8**, 13917 (2017).

[9] M. Först, C. Manzoni, S. Kaiser, Y. Tomioka, Y. Tokura, R. Merlin, and A. Cavalleri, Nonlinear phononics as an ultrafast route to lattice control, Nat. Phys. **7**, 854 (2011).

[10] S. Iwai, M. Ono, A. Maeda, H. Matsuzaki, H. Kishida, H. Okamoto, and Y. Tokura, Ultrafast optical switching to a metallic state by photoinduced Mott transition in a halogen-bridged nickel-chain compound, Phys. Rev. Lett. **91**, 057401 (2003).

[11] H. Okamoto, H. Matsuzaki, T. Wakabayashi, Y. Takahashi, and T. Hasegawa, Photoinduced metallic state mediated by spin-charge separation in a one-dimensional organic Mott insulator, Phys. Rev. Lett. **98**, 037401 (2007).

[12] N. Dean, J. C. Petersen, D. Fausti, R. I. Tobey, S. Kaiser, L. V. Gasparov, H. Berger, and A. Cavalleri, Polaronic conductivity in the photoinduced phase of $1T$-TaS_2. Phys. Rev. Lett. **106**, 016401 (2011).

[13] D. Fausti, R. I. Tobey, N. Dean, S. Kaiser, A. Dienst, M. C. Hoffmann, S. Pyon, T. Takayama, H. Takagi, and A. Cavalleri, Light-induced superconductivity in a stripe-ordered cuprate, Science **331**, 189 (2011).

[14] M. Mitrano, A. Cantaluppi, D. Nicoletti, S. Kaiser, A. Perucchi, S. Lupi, P. Di Pietro, D. Pontiroli, M. Riccò, S. R. Clark *et al.*, Possible light-induced superconductivity in K_3C_{60} at high temperature, Nature (London) **530**, 461 (2016).

[15] M. Buzzi, D. Nicoletti, S. Fava, G. Jotzu, K. Miyagawa, K. Kanoda, A. Henderson, T. Siegrist, J. A. Schlueter, M.-S. Nam *et al.*, Phase diagram for light-induced supercoductivity in κ-$(ET)_2$-X, Phys. Rev. Lett. **127**, 197002 (2021).

[16] S. Mor, M. Herzog, D. Golež, P. Werner, M. Eckstein, N. Katayama, M. Nohara, H. Takagi, T. Mizokawa, C. Monney *et al.*, Ultrafast electronic band gap control in an excitonic insulator, Phys. Rev. Lett. **119**, 086401 (2017).

[17] E. N. Glezer, Y. Siegal, L. Huang, and E. Mazur, Laser-induced band-gap collapse in GaAs, Phys. Rev. B **51**, 6959 (1995).

[18] D. Wegkamp, M. Herzog, L. Xian, M. Gatti, P. Cudazzo, C. L. McGahan, R. E. Marvel, R. F. Haglund, Jr. A. Rubio, M. Wolf, Instantaneous band gap collapse in photoexcited monoclinic VO_2 due to photocarrier doping, Phys. Rev. Lett. **113**, 216401 (2014).

[19] P. W. E. Smith, S. D. Benjamin, and H. S. Loka, Tailoring of trap-related carrier dynamics in low-temperature-grown GaAs, Appl. Phys. Lett. **71**, 1156 (1997).

[20] N. Yoshikawa, H. Suganuma, H. Matsuoka, Y. Tanaka, P. Hemme, M. Cazayous, Y. Gallais, M. Nakano, Y. Iwasa, and R. Shimano, Ultrafast switching to an insulating-like metastable state by amplitudon excitation of a charge density wave, Nat. Phys. **17**, 909 (2021).

[21] P.W. Anderson, Absence of diffusion in certain random lattices, Phys. Rev. **109**, 1492 (1958).

[22] M. Filoche and S. Mayboroda, Universal mechanism for Anderson and weak localization, Proc. Natl. Acad. Sci. USA **109**, 14761 (2012).

[23] L. Cario, A. Meerschaut, B. Corraze, and O. Chauvet, Determination of the modulated structure of the misfit layer compound $(LaS)_{1.196}VS_2$, Mater. Res. Bull., **40**, 125 (2005).

[24] A. Meerschaut, *Incommensurate Sandwiched Layered Compounds* (Trans Tech Publications, Zurich, 1992).

[25] G. A. Wiegers, Misfit layer compounds: Structures and physical properties, Prog. Solid State Chem. **24**, 1 (1996).

[26] T. Kondo, K. Suzuki, T. Enoki, H. Tajima, and T. Ohta, Conduction and localization in incommensurate misfit layer compounds, J. Phys. Chem. Solids **57**, 1105 (1996).

[27] L. Cario, B. Corraze, A. Meerschaut, and O. Chauvet, Dielectric breakdown and current switching effect in the incommensurate layered compound $(LaS)_{1.196}VS_2$, Phys. Rev. B **73**, 155116 (2006).

[28] V. Ta Phuoc, V. Brouet, B. Corraze, E. Janod, M. Zaghrioui, and L. Cario, Relation between thermally induced structural distortions and electronic properties of the layered misfit chalcogenide $(LaS)_{1.196}VS_2$, J. Phys. Chem. C **118**, 19273 (2014).

[29] V. Brouet, J. Mauchain, E. Papalazarou, J. Faure, M. Marsi, P. H. Lin, A. Taleb-Ibrahimi, P. Le Fèvre, F. Bertran, L. Cario *et al.*, Ultrafast filling of an electronic pseudogap in an incommensurate crystal, Phys. Rev. B **87**, 041106(R) (2013).

[30] T. Kondo, K. Suzuki, and T. Enoki, Conduction properties of incommensurate misfit layer compounds $(CeS)_{1.19}(TiS_2)_n (n = 1, 2)$, J. Phys. Soc. Jpn. **64**, 4296 (1995).

[31] M. Imada, A. Fujimori, and Y. Tokura, Metal-insulator transitions, Rev. Mod. Phys. **70**, 1039 (1998).

[32] A. Ino, T. Okane, S.-I. Fujimori, A. Fujimori, T. Mizokawa, Y. Yasui, T. Nishikawa, and M. Sato, Evolution of the electronic structure from electron-doped to hole-doped states in the two-dimensional Mott-Hubbard system $La_{1.17-x}Pb_xVS_{3.17}$, Phys. Rev. B **69**, 195116 (2004).

[33] D. Boschetto, E. G. Gamaly, A. V. Rode, B. Luther-Davies, D. Glijer, T. Garl, O. Albert, A. Rousse, and J. Etchepare, Small atomic displacements recorded in bismuth by the optical reflectivity of femtosecond laser-pulse excitations, Phys. Rev. Lett. **100**, 027404 (2008).

[34] See Supplemental Material at http://link.aps.org/supplemental/10.1103/PhysRevB.108.134306 for details on the experimental setups, sample growth, DFT calculations, and a comprehensive description of the theoretical approach used to fit the experimental results. It also presents experimental results using pump and probe pulses centered at 1.7 μm (0.73 eV) and 1.5 μm (0.83 eV), respectively, as well as equilibrium ellipsometry measurements around 1.5 μm at three different temperatures.

[35] Z. Lin, L. V. Zhigilei, and V. Celli, Electron-phonon coupling and electron heat capacity of metals under conditions of strong electron-phonon nonequilibrium, Phys. Rev. B **77**, 075133 (2008).

[36] D. Boschetto, M. Weis, J. Zhang, J. Caillaux, N. Nilforoushan, G. Lantz, B. Mansart, E. Papalazarou, N. Moisan, D. Grieger *et al.*, Reply to: Ultrafast evolution and transient phases of a prototype out-of-equilibrium Mott-Hubbard material, Nat. Commun. **10**, 4035 (2019).